WARSAW UNIVERSITY OF TECHNOLOGY Index 351733
FACULTY OF CIVIL ENGINEERING
COMMITTEE FOR CIVIL AND WATER ENGINEERING
POLISH ACADEMY OF SCIENCES ISSN 1230-2945

DOI: 10.24425/ace.2023.145268

ARCHIVES OF CIVIL ENGINEERING

Vol. LXIX ISSUE 2 2023

pp. 291 –309

Research paper

A study of landslide body control of black bovine cave copper ore mining and beneficiation project

Hanhui Wu[1]

Abstract: Landslide is a common geological disaster which causes huge losses to people's properties and national economic development. How to prevent and control landslides has become an important issue. This article introduces the geological and geographical environment of the landslide body, analyzes the basic characteristics of the landslide, calculates the landslide stability based on the ultimate equilibrium theory-based transfer coefficient method, discusses the development trend of the landslide and comes up with corresponding control schemes by taking the landslide body of Black Bovine Cave Copper Ore Mining & Beneficiation Project as example. It is found that the control scheme – "anti-slide pile + retraining wall + baffle + anchor cable" can be used to effectively prevent and control the geological disaster according to calculation. The study results can provide a reference for landslide body control.

Keywords: black bovine cave copper ore, landslide body, stability analysis, control scheme

[1]Associate Professor, PhD., Civil Engineering, School of Civil Engineering, Chongqing Chemical Industry Vocational College, 400020 Chongqing, China, e-mail: jgxy@cqcivc.edu.cn, ORCID: 0000-0002-2223-4487

1. Introduction

Landslide refers to the natural phenomenon that soils or rocks on the slopes are affected by factors such as rain soaking, earthquake and man-made cut slope and then slide down the slopes along a certain weak surface or weak zone in a whole or scattered manner under the action of gravity. The soil masses or rock masses that slide down the slopes are called as landslide bodies. Many scholars have studied landslide prevention and control as well as landslide body control, with many results achieved. Rosser et al. [1] developed the New Zealand landslide database and provided actual data for landslide disaster and risk assessment. Marin et al. [2, 3] studied the influences of basin shape parameters on the physical based rainfall threshold for shallow landslides, and discussed the applicability of deterministic and probabilistic physics-based landslide modeling in the data-poor environment of Andes Mountains in Colombia. Gorum et al. [4] found that the regional differences in terrain and climatic environments were essential for controlling the pattern of fatal landslides. Ko et al. [5] investigated the frequency of landslides in Hong Kong. Rana et al. [6] proposed a method of classifying landslide triggering mechanisms in the existing inventory. Patton et al. [7] studied the influences of melting frozen soil on the formation of landslides. Lombardo et al. [8] classified model results based on the landslide intensity and sensitivity. Kumar et al. [9] evaluated the slope failure mechanism, dam size and dam stability to learn about the potential landslide process. Rezaei et al. [10] determined the three-dimensional geometric structure of landslide with electrical resistivity tomography.

It can be concluded from the current study status that how to effectively analyze and control landslide bodies is of great significance [11, 12]. Therefore, the objective of this research article is to analyze the geographical and geological environment of the landslide body, evaluate the basic characteristics and stability of the landslide, and propose the corresponding control scheme by taking the landslide body of Black Bovine Cave Copper Ore Mining & Beneficiation Project as example. Relevant studies can provide a reference for landslide body control.

2. Project overview

The 1500 t/d Black Bovine Cave Copper Ore Mining & Beneficiation Project of Jiulong YalongJiang Mining Co., Ltd., located in Jianglang Village, Kuiduo Township, Jiulong County. The proposed site features denudation landform and eroded accumulation landform of mid-high mountain structure, sloped landform, low relief in the south and high relief in the north, a relevant elevation difference of 340 m, and a natural slope of about 25°–35°. According to the site planning and design of the general layout plan, the sloped site is planned with multiple building platforms. Due to continuous rainfalls during the site leveling construction, the excavated slope deformed, the slope at the rear edge of No. 1–2 retaining wall collapsed, and the newly built No. 1–2 and No. 2–2 retaining walls cracked. Fissures of ground surfaces were observed in areas such as the proposed crude ore bin, coarse crushing chamber, medium crushing chamber and east side of No. 2–2 retaining

wall. The anti-slide pile protection walls excavated for No. 4–2 retaining wall and No. 6 retraining wall (sheet-pile retaining wall) under construction cracked, and the fore shaft of the anti-slide pile inclined to form a landslide, threatening the safety of proposed dressing plant.

The exploration area is located in the proposed dressing plant of Jiulong YalongJiang Mining Co., Ltd. Its site features denudation landform and eroded accumulation landform of mid-high mountain structure, sloped landform, low relief in the south and high relief in the north, and a natural slope of about 25°–35°. The landslide is about 170 m long from south to north and about 100–150 m wide from east to west. The landslide area is about 2.46×10^4 m^2 with the main sliding direction of 181°. The sliding surface is buried by 9.7 to 17.5 m and averagely about 13.0 m. The landslide volume is about 32.0×10^4 m^3, and the landslide is a medium-sized middle-level pull-type landslide.

3. Geographical and geological environment

3.1. Geographical location and transportation

The landslide of the 1500 t/d Black Bovine Cave Copper Ore Mining & Beneficiation Project of Jiulong YalongJiang Mining Co., Ltd. The exploration area is located on a high mountain and connected by a mountain road with relatively convenient transportation, as shown in Fig. 1.

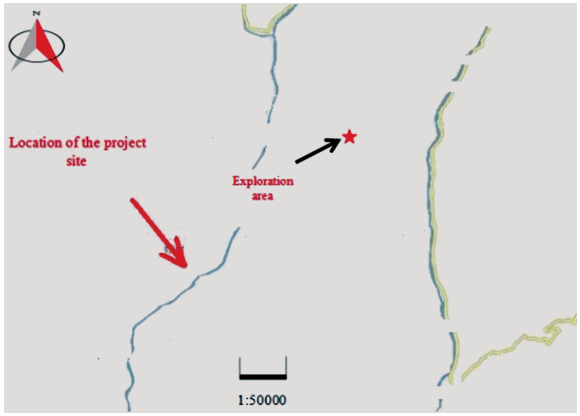

Fig. 1. Traffic location map

3.2. Geological environment

The site of the 1500 t/d Black Bovine Cave Copper Ore Mining & Beneficiation Project of Jiulong YalongJiang Mining Co., Ltd. in Sichuan Province is located in Jianglang Village, Kuiduo Township, Jiulong County. At a straight-line distance of 1.5 km away

from the southwest side of the Liwu copper deposit plant area and connected by roads and village roads, it is provided with convenient transportation. The landslide area has an elevation of between 2738–2840 m, a relative elevation difference of 102 m and a natural slope of about 25°–35°. Its site features denudation landform and eroded accumulation landform of mid-high mountain structure, sloped landform, and low relief in the south and high relief in the north. Before the landslide occurs, the de-sloped landslide site is planned into multiple levels of platforms with elevations of 2814.80, 2802.00, 2784.00, 2761.80, 2756.00, 2748.00 and 2735.00 from top to bottom respectively. Retaining walls (No. 5 retaining walls) or sheet-pile retaining walls (No. 2, No. 4, No. 6 and No. 9 retaining walls) are used to support the slopes between these platforms. The proposed retaining walls are 2–6 m high and designed with the structure of rubble concrete and stone blocks with cement mortar. The proposed sheet-pile retaining walls are all 12–30 m long cantilever piles. The cantilever sections are 5.8–17 m high and usually provided with 2 to 4 rows of anchor cables. The site undergoes levelling construction, and the slope is mostly stepped.

According to the surface survey and drilling, the lithology revealed in the site includes Quaternary Holocene Qml and Quaternary Lower Pleistocene Qedol. The lithological characteristics of each stratum are described below:

Plain fill

Gray, gray-brown, and mainly composed of silty clay, silt, silty sand and mica schist gravel, Qml is used for backfilling in site leveling. It is newly filled earth. Qml is slightly wet and loose. It is mainly distributed on the surface layer of the excavated platform and in the 35 KV substation area. Except borehole ZK1 and exploratory wells TJ2 and TJ3, all other boreholes are revealed, with a revealed thickness of 0.5–2.4 m.

Quaternary Lower Pleistocene Qedol

Qedol can be divided into four sub-strata of silty clay with gravels, gravel-containing silt with silty sand, gravelly soil, and soil with crushed stones according to the particle size content. The strata mentioned above are interbedded.

Silty clay with gravels: Yellow-gray, gray-brown, light gray-green, silty sand with silt, and generally containing 15%–30% of mica schist gravels and breccias. Particle size composition of gravels and breccias: 2–20 mm (about 5%–10%), 20–60 mm (about 5%–10%) and 60–200 mm (about 5%–10%), which are unevenly distributed and locally enriched. It is free of dilatance; with glossy aspect, dry strength and moderate toughness; and slightly wet to wet and plastic to hard plastic. All are revealed in the site, with a revealed thickness of 0.7–8.28 m.

Gravel-containing silt with silty sand: Yellow-brown, gray, gray-brown, and generally containing 15%–35% of mica schist gravels and breccias. Particle size composition of gravels and breccias: 2–20 mm (about 5%–10%), 20–60 mm (about 5%–15%), 60–200 mm (about 5%–15%), and $\varphi > 200$ mm (about 0–5%), which are unevenly distributed and locally enriched. It is of dry strength and low toughness, slight wet to very wet, and slightly dense to medium dense. Except boreholes ZK2 and ZK5, all other boreholes are revealed, with a revealed thickness of 1.1–9.5 m.

Gravelly soil: Gray, gray-brown, particle size composition: 20–60 mm (about 5%–40%), 60–200 mm (about 10%–45%), and φ > 200 mm (about 0–15%); Rocks are mostly mica schist, sub-angular, and hard to very hard. It is filled with silt and silty sand, slightly wet to wet, and slightly dense to medium dense. Except boreholes ZK3, ZK7 and ZK8, all other boreholes are revealed, with a revealed thickness of 0.8–13.4 m.

Soil with crushed stones: Gray, gray-brown, particle size composition: 20–60 mm (about 0%–15%), 60–200 mm (about 10%–30%), and φ > 200 mm (about 20%–40%); Rocks are mostly mica schist, sub-angular, and hard to very hard. It is filled with silty clay, silt and silty sand, slightly wet to wet, and medium dense. All are revealed in the site, with a revealed thickness of 3.5–24.73 m.

3.3. Geological structure and neotectonic movement

According to the local geological structure, the site is located in the southern section of the Jianglang anticline, a secondary structure of the Songpan-Garzi trough fold system, and the axis of the regional Jianglang anticline passes through the east side of the site. The Jinping Mountain deep fault is 7 km away in the east of the site. It is huge in scale, strikes from north to east, and slopes from south to east with a dip angle of 70°–82°. There is a compresso-crushed zone with a varying width along the fault. The fault cliff extends for several kilometers. It is a normal fault. The Mozi Gully fault set is located in the Mozi Gully area 8 km away in the southwest of the site. It includes three parallel faults striking in the NNW direction. Sloping from north to east with a dip angle of 70°–85°, these faults are high-angle thrust faults.

4. Basic characteristics and stability evaluation of the landslide

4.1. Deformation and failure characteristics

The landslide is located in the proposed dressing plant of Jiulong YalongJiang Mining Co., Ltd. Its site features sloped landform, low relief in the south and high relief in the north, and a natural slope of about 25°–35°. According to the site planning and design of the general layout plan, the sloped site is planned with multiple building platforms. Due to continuous rainfalls in the site leveling construction, the excavated slope deformed to form the landslide, threatening the safety of the proposed dressing plant. It is proposed to build No. 9 retaining wall (see Fig. 2) at the leading edge of the landslide. Its deformation is mainly reflected by the collapse of the excavated slope inside the proposed retaining wall (see Fig. 3). There are many cracks in the landslide body due to the sliding of the landslide. The characteristics of typical cracks in the landslide are as shown in Table 1.

No. 4–2 and No. 6 retaining walls (sheet-pile retaining walls) are being built in the middle of the landslide. When anti-slide pile holes were excavated, the protective wall mostly cracked in the 10.0–18.0 areas of pile bodies, and the fore shafts of anti-slide piles

Fig. 2. Photo of No. 9 retaining wall at the leading edge of the landslide

Fig. 3. Collapsed slope inside No. 9 retaining wall

Table 1. Characteristics of typical cracks of the landslide

Type	Location of crack	Crack No.	Description of crack characteristics
Tension crack	Migrant laborer houses at the rear edge of the cracked landslide, rear edges of crude ore bin and coarse crushing chamber, and east side of the proposed No. 5 retaining wall	L1–L6	Cracks L1 and L2 are 12–20 m long, 2–6 cm wide and visibly 0.2–0.5 m deep with a strike of 82°–85°. Cracks L3 to L5 are 12–16 m long, 1–5 cm wide as investigated and visibly 0.2–0.5 m deep with a strike of 75°–108°. Since the exploration period is in the rainy season, these cracks have been scoured by the rainwater and buried by slurry. Crack L6 is about 12 m long with a strike of 75°. It has been scoured by the rainwater and buried by the slurry
Shear crack	West and northwest sides of the medium crushing chamber, east side of No. 1–2 retaining wall, and east side of No. 2–2 retaining wall	L7–L15	Cracks L7 and L8 are 6–13 m long and 0.5–3 cm wide with a strike of 165°–172°. Crack L9 is 7 m long and 2 cm wide with a strike of 188°. Crack L10 is 15 m long and 1–3 cm wide with a strike of 188°. Cracks L11 and L12 are 5–8 m long and 0.5-3 cm wide with a strike of 142°–155°. Cracks L13 to L15 are 3–5 m long and 1–4 cm wide with a strike of 153°–169°. These cracks are dense and parallel

of No. 4 and No. 6 retaining walls were obviously inclined and sank. In order to prevent the landslide from causing severe landslides, the construction unit has immediately backfilled the excavated anti-slide pile holes. The 1.0–3.5 m high obvious back wall can be observed at the rear edge of the landslide. The retaining wall for the road at the rear edge of the landslide is deformed and damaged, and the cracks in the wall body have been basically penetrated. No. 4–2 and No. 6 retaining walls (sheet-pile retaining walls) are being built in the middle of the landslide. When anti-slide pile holes were excavated, the protective wall mostly cracked in the 10.0–18.0 areas of pile bodies, and the fore shafts of anti-slide piles

of No. 4 and No. 6 retaining walls were obviously inclined and sank. In order to prevent the landslide from causing severe landslides, the construction unit has immediately backfilled the excavated anti-slide pile holes (see Fig. 4). The 1.0–3.5 m high obvious back wall can be observed at the rear edge of the landslide (see Fig. 5). The retaining wall for the road at the rear edge of the landslide is deformed and damaged, and the cracks in the wall body have been basically penetrated.

Fig. 4. Backfill of anti-slide pile holes with pebbles

Fig. 5. Back wall of the landslide

4.1.1. Material composition

According to the ground survey and exploration, the strata in the landslide area include Quaternary Holocene Qml (Q_4^{ml}) and Quaternary Lower Pleistocene Qedol (Q_1^{col+dl}). The potential slip mass is composed of gravelly soil, the potential sliding zone is mainly composed of the weak intercalated layer of the rock-soil contact zone, and the potential sliding bed is composed of gravelly soil.

1. Characteristics of potential slip mass

The slip mass is mainly composed of the Lower Pleistocene Qedol (Q_1^{col+dl}), including silty clay with gravels, gravel-containing silt with silty sand, gravelly soil, and soil with crushed stones. The stratum structure of the slip mass is dominated by gravelly soil and soil with crushed stones. Except distributed on the surface, silty clay with gravels and gravel-containing silt with silty sand mainly appear as thin layers and interlayers. Silty clay with gravels: usually containing 15%–30% of mica schist gravel and breccia, it is slightly wet to wet and plastic to hard plastic. Gravel-containing silt with silty sand: with silty clay and silt and usually containing 15%–35% of mica schist gravel and breccia, it is slightly wet to wet and slightly dense to medium dense. Gravelly soil: particle size composition: 20–60 mm (about 5%–40%), 60–200 mm (about 10%–45%), and φ >200 mm (about 0–15%). Rocks are mostly mica schist. It is filled with silt and silty sand, slightly wet to wet, and slightly dense to medium dense soil with crushed stones: Gray, gray-brown, and particle size composition: 20–60 mm (about 0%–15%), 60–200 mm (about 10%–30%),

and $\varphi > 200$ mm (about 20%–40%); Rocks are mostly mica schist. It is filled with silty clay, silt and silty sand, slightly wet to wet, and medium dense.

2. Characteristics of potential sliding zone

Drilling reveals that the sliding zone is mainly located in the Quaternary Qedol. The soil in the sliding zone is silty clay with gravels (see Fig. 6) with a thickness of 0.3–0.7 m. It is slightly wet to wet, and plastic. The soil in the sliding zone is slightly squeezed with crumpled traces.

Fig. 6. Core of the sliding zone

3. Characteristics of potential sliding bed

The sliding bed is mainly composed of Quaternary Qedol gravelly soil and soil with crushed stones. According to the heavy dynamic penetration test, the range of hammering times N after the gravelly soil is corrected is 6.4–18.2 with an average of 10.741 times/10 cm. The CV is $\delta = 0.29$, showing low compressibility. Boreholes show that the sliding bed is usually buried by 9.7–17.5 m and that the landslide is thicker in the middle with an average depth of about 13.0 m.

4.1.2. Formation mechanism

A steep slope is at the trailing edge of the slope with a steep terrain and a thick covering layer, and the terrain in the slope area is steep. It can be concluded from the comprehensive analysis of terrain, landform and stratum lithology characteristics of the whole area that the formation of the unstable slope is most closely related to the terrain and stratum.

Many years ago, filling materials such as gravels and cohesive soil were formed in the pores of the collapsed blocks at the rear edge of the slope under the action of weathering, providing a necessary material foundation for the formation of the unstable slope. It is well known that it is hard for pure crushed stones to slide. Only the crushed stones containing a certain amount of fine-grained soil can accumulate water which will in turn soften the soil. The loose accumulation formation in the slope area is mainly composed of siltstone, crushed stone and thin-bedded slate. It is easy for the thin-bedded slate to weather into fine-grained soil. The exploration zone is located in the mountainous area with frequent

rainfalls, providing sufficient "lubricant" for the instability of the slope. A gully is shaped at the toe of the slope. Due to scouring and cut by the ravine, the terrain at the leading edge of the slope becomes steep, providing a wide deformation space for the instability of slope sediments. After materials have been reserved for a long time, the rainstorm will cause the accumulation body on the slope to locally deform to form an unstable slope when material conditions, terrain conditions and other preconditions are met.

4.2. Stability analysis and evaluation of landslide

4.2.1. Physico-mechanical properties of rock and soil masses

According to the result data at the control engineering site, the specific design parameters of each type of rock and soil masses are determined as shown in Table 2.

Table 2. Main physical and mechanical indicators of rock and soil masses

Name \ Indicator	Weight (kN/m^3)	Compression modulus (MPa)	Cohesive force (kPa)	Internal Friction Angle (°)	Characteristic value of bearing capacity (kPa)	Friction coefficient of basement on concrete	Characteristic value of binding strength of rock and soil masses and anchorage body (kPa)	Proportional coefficient of horizontal resistance factor of foundation (MN/m^4)
Plain fill	19.0	/	/	/	/	/	/	/
Silty clay with gravels	19.5	10	26	22	160	0.30	25	20
Gravel-containing silt with silty sand	19.5	12	10	28	180	0.30	35	30
Gravelly soil	20.5	18	10	35	300	0.40	90	80
Soil with crushed stones	21.5	25	10	39	450	0.45	120	100
Soil in the sliding zone	20.5	/	25.8	21.7	/	/	/	/

4.2.2. Stability analysis

The potential sliding surface shape of the slope is in the shape of a fold line. According to the requirements of literature [13], the stability of the unstable slope shall be quantitatively analyzed and calculated by the limit equilibrium theory-based transfer coefficient method.

The stability coefficient shall be calculated according to the following calculation formula:

$$F_s = \frac{\sum_{i-1}^{n-1}\left(W_i \cos\alpha_i \tan\varphi_i + C_i L_i\right)\prod_{j=i}^{n-1}\psi_j\Big) + Rn}{\sum_{i=1}^{n-1}\left[W_i \sin\alpha_i \prod_{j=i}^{n-1}\psi_j\right] + Tn} \tag{4.1}$$

where: W_i is the weight of the i-th block (kN/m); α_i is the dip angle of the sliding surface of the i-th block (°); φ_i is the internal friction angle of the i-th block (°); C_i is the cohesive force of the i-th block (kPa); L_i is the length of the sliding surface of the i-th block (m); ψ_j is the transfer coefficient when the surplus sliding force of the i-first section is transferred to the i-th section, that is: $\psi_j = \cos(\alpha_{i-1} - \alpha_i) - \sin(\alpha_{i-1} - \alpha_i) \cdot \tan\phi_i$; $Rn = Wn\cos\alpha n \tan\varphi_i + CnLn$; $Tn = Wn \sin\alpha n$.

Excess thrust calculation formula:

$$E_i = K_s W_i \sin\alpha_i + \psi_i E_{i-1} - W_i \cos\alpha_i \tan\varphi_i - C_i L_i \tag{4.2}$$

where: K_s is the anti-slide safety coefficient, which is calculated as 1.15, 1.05 and 1.05 respectively; Other symbols are the same as the those of the stability coefficient calculation formula.

According to the arrangement of the exploration work and the actual conditions of the unstable slope, No. 1–1, No. 2–2 and No. 3–3 sections are used to calculate the overall stability in section calculation, see Fig. 7. The weak interlayer is taken as the potential sliding surface, which is in the shape of a fold line.

Basic loads include: the basic loads acting on the slope, such as the dead weight of the slope, the weight of the proposed building, and the static pressure of groundwater formed by rainfall infiltration; and the dead weight of the potential slip mass, which is calculated as the natural weight in the natural conditions and considered as saturated unit weight in the rainstorm conditions. The seismic acceleration is considered to be 0.20 g in the seismic conditions.

Calculation conditions are divided into three types: (1) natural conditions: dead weight + groundwater; (2) rainstorm conditions: dead weight + rainstorm + groundwater; (3) seismic conditions: dead weight + earthquake + groundwater. And Fig. 8 is the 1–1 section support scheme.

According to the objects endangered by the unstable slope, number of people affected, economic loss and construction difficulty, the prevention and control engineering grade is classified into Grade II and the anti-slide stability safety coefficient is 1.15 (in natural conditions), 1.10 (in rainstorm conditions) and 1.10 (in seismic conditions).

It can be concluded from the comprehensive analysis of the morphological and structural characteristics of the slope and the characteristics of the stratum exposed by the excavation that the potential sliding surface of the unstable slope is a weak interlayer, which is in the shape of a fold line, steep in the front and gentle at the back. It can also be concluded

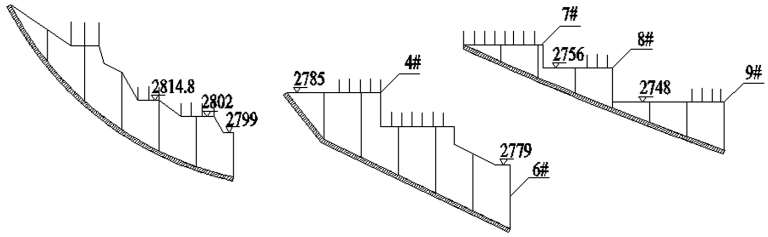

(a) Sliding surface A (b) Sliding surface B (c) Sliding surface C

1–1 section

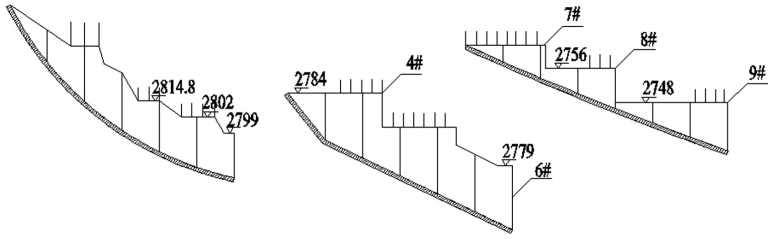

(a) Sliding surface A (b) Sliding surface B (c) Sliding surface C

2–2 section

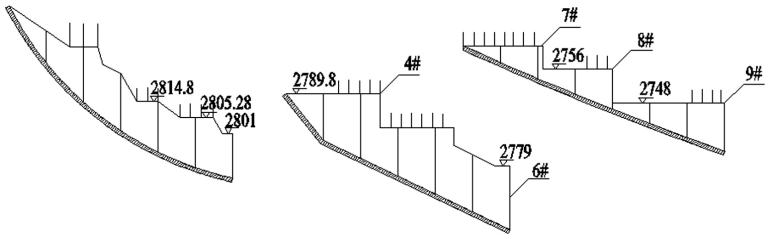

(a) Sliding surface A (b) Sliding surface B (c) Sliding surface C

3–3 section

Fig. 7. Typical sections

from the analysis of terrain and deformation characteristics that if the slope is unstable, its possible instability modes include the overall instability before site leveling and the multi-level platform instability after site leveling.

1. Two calculation models have been established according to the combination of the potential sliding surface mentioned above, the determination of shear outlet and the deformation characteristics of the slope: pre-site leveling failure mode and post-site leveling failure mode.

The weight value is comprehensively determined according to the heavy weight test on the site, the indoor test results and the soil-rock ratio of the accumulation layer on the slope. The soil in the potential slip mass is the gravelly soil with a soil-rock ratio of about 4:6. Given the loose structure of the gravelly soil, there are some gaps in the soil mass. It is

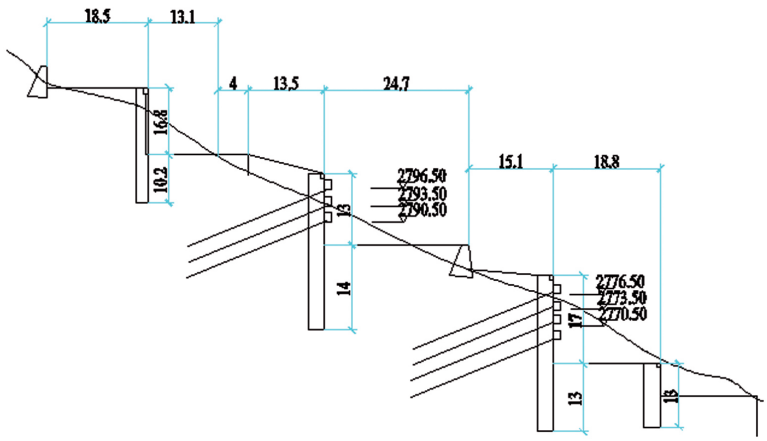

Fig. 8. 1–1 section support scheme

determined according to the regional experience that the natural weight and saturated unit weight of the slip mass are $\gamma = 20.5$ kN/m^3 and $\gamma = 21.5$ kN/m^3 respectively.

No. 1–1, No. 2–2 and No. 3–3 sections are chosen for back calculation. The landslide is basically stable at present. A safety coefficient of $K = 1.10$ is taken for back calculation, with the calculation results as shown in Table 3.

Table 3. Back calculation results of C/φ value

Section No.	Natural conditions		Saturated conditions in rainstorm	
	Cohesive force (kPa)	Internal Friction Angle (°)	Cohesive force (kPa)	Internal Friction Angle (°)
1–1	25.4	21.5	22.9	20.5
2–2	25.8	21.7	23.3	20.7
3–3	26.6	22.6	24.0	21.6
Average	26.0	21.9	23.6	20.9

According to the test data of the samples taken during the exploration, the cohesive force obtained by natural quick shear of the oil in the sliding zone is 23–28 kPa, with an average of 25.833 kPa. The internal friction angle is 20°–23.5°, with an average of 21.667°. The cohesive force obtained by saturated fast shear is 20–26 kPa, with an average of 23.167 kPa. The internal friction angle is 19°–22.5°, with an average of 20.583°. Comparing the two values, the C value obtained by natural fast shear test of the soil taken form the sliding zone is slightly higher than that obtained by inversion, and the value obtained by saturated fast shear test is slightly lower than that obtained by inversion. According to the test data and in combination with similar engineering experience and the inversion analysis results, the physical and mechanical indicators of the soil in the sliding zone soil are selected as

follows: C = 25.8 kPa and φ = 21.7° (in the natural conditions), and = 23.3 kPa and φ = 20.7° (in the saturated conditions).

According to the working conditions, parameters and calculation models mentioned above, the transfer coefficient method is used to quantitatively calculate the stability of the slope in each failure mode:

1. Pre-site leveling stability calculation

In working condition I: Dead weight + groundwater is the design working condition, and the engineering design safety coefficient is 1.15. In working condition II: Dead weight + rainstorm + groundwater is the check working condition, and the engineering design safety coefficient is 1.10. In working condition III: Dead weight + earthquake + groundwater is the check working condition, and the engineering design safety coefficient is 1.10. After calculation, the current stability of the landslide and the thrust calculation results based on the corresponding safety coefficient of each working condition are listed in Table 4.

Table 4. Current stability and thrust calculation results of landslide

Section No.	Calculation conditions	Stability coefficient (F)	Steady state	Safety coefficient (K_s)	Surplus sliding force (kN/m)
1–1′	Working condition I	1.113	Basically stable	1.15	537.477
	Working condition II	1.031	Less stable	1.10	1079.726
	Working condition III	1.053	Less stable	1.10	747.135
2–2′	Working condition I	1.099	Basically stable	1.15	885.572
	Working condition II	1.02	Less stable	1.10	1477.977
	Working condition III	1.038	Less stable	1.10	1149.625
3–3′	Working condition I	1.055	Basically stable	1.15	1624.207
	Working condition II	0.977	Unstable	1.10	2215.747
	Working condition III	1.0	Less stable	1.10	1821.816

2. Post-site leveling stability calculation

According to the parameters mentioned above, the transfer coefficient method is used to calculate the stability and thrust of each secondary sliding surface mentioned above. In calculation, a load of 150 kN/m is considered for the proposed building, and a load of Class 20 vehicle load is considered for the road, with the calculation results as shown in Table 5.

The stable status of the slope shall be determined based on the stability coefficient according to Table 6.

It can be concluded from the calculation results that the quantitative calculation results are consistent with the macro judgement results and also in line with the actual situation on the site, showing that the establishment of the calculation model and the parameter values are reasonable.

It can be concluded from Table 6 that the current landslide has a stability coefficient of 1.055–1.113 and is basically stable in working condition I; has a stability coefficient of 0.977–1.031 and is unstable to less stable in working condition II; and has a stability coefficient of 1.0–1.053 and is less stable in working condition III. The landslide has a low stability coefficient in working conditions II and III, showing that the landslide may be exacerbated in rainstorms or earthquakes.

It can be found from Table 5 and Table 6 that the landslide has a stability coefficient of 0.849–1.354 and is unstable to stable in working condition I after site leveling. The sliding surface B has a low stability coefficient and is unstable. The sliding surface C has a high stability coefficient and is stable. The stability coefficient is 0.795–1.262 in working

Table 5. Stability and thrust calculation results of the landslide after site leveling

Section No.	No. of sliding surface	Calculation conditions	Stability coefficient (F)	Steady state	Safety coefficient (K_s)	Surplus sliding force (kN/m)
1–1	Sliding surface A	Working condition I	1.067	Basically stable	1.15	819.551
		Working condition II	0.995	Unstable	1.10	1091.899
		Working condition III	1.022	Less stable	1.10	808.837
	Sliding surface B	Working condition I	0.849	Unstable	1.15	1747.604
		Working condition II	0.795	Unstable	1.10	1856.431
		Working condition III	0.817	Unstable	1.10	1670.862
	Sliding surface C	Working condition I	1.318	Stable	1.15	/
		Working condition II	1.234	Stable	1.10	/
		Working condition III	1.269	Stable	1.10	/

Continued on next page

Table 5 – *Continued from previous page*

Section No.	No. of sliding surface	Calculation conditions	Stability coefficient (F)	Steady state	Safety coefficient (K_s)	Surplus sliding force (kN/m)
2–2	Sliding surface A	Working condition I	1.033	Less stable	1.15	966.339
		Working condition II	0.959	Unstable	1.10	1225.487
		Working condition III	0.985	Unstable	1.10	1001.984
	Sliding surface B	Working condition I	0.953	Unstable	1.15	1159.240
		Working condition II	0.891	Unstable	1.10	1271.361
		Working condition III	0.918	Unstable	1.10	1107.812
	Sliding surface C	Working condition I	1.300	Stable	1.15	/
		Working condition II	1.216	Stable	1.10	/
		Working condition III	1.255	Stable	1.10	/
3–3	Sliding surface A	Working condition I	0.959	Unstable	1.15	1520.600
		Working condition II	0.893	Unstable	1.10	1748.528
		Working condition III	0.919	Less stable	1.10	1503.596
	Sliding surface B	Working condition I	0.993	Unstable	1.15	1043.931
		Working condition II	0.930	Unstable	1.10	1198.170
		Working condition III	0.954	Unstable	1.10	1007.437
	Sliding surface C	Working condition I	1.354	Stable	1.15	/
		Working condition II	1.262	Stable	1.10	/
		Working condition III	1.299	Stable	1.10	/

Table 6. Ratings of stable status

Stability coefficient (F_s)	$F_s < 1.00$	$1.00 \leq F_s < 1.05$	$1.05 \leq F_s < 1.15$	$F_s \geq 1.15$
Steady state	Unstable	Less stable	Basically stable	Stable

Note: F_s is the stability coefficient.

condition II. Except that the sliding surface C has a stability coefficient of over 1 and is stable, all other sliding surfaces are unstable. The stability coefficient is 0.817–1.299 in working condition III. The sliding surface B of No. 1–1 section as well as the sliding surfaces A and B of No. 2–2 and 3–3 sections have a stability coefficient of smaller than 1 and are unstable. The sliding surface C has a stability coefficient of bigger than 1 and is stable, while other sliding surfaces are less stable. Generally speaking, sliding surfaces A and B of each section have a poor stability, i.e. it is highly feasible to cut out the landslide from No. 4 and No. 6 retaining walls. However, the sliding surface C has a good stability.

4.2.3. Development trend of the landslide

The landslide is located in the proposed dressing plant of Jiulong YalongJiang Mining Co., Ltd. Its site features denudation landform and eroded accumulation landform of mid-high mountain structure, sloped landform, and a natural slope of about 25°–35°. Due to the requirements of engineering construction, the site is being levelled. The slope is excavated to form multiple levels of platforms. The platform slopes after excavation isn't supported in time. The site leveling construction is carried out in the rainy season with concentrated rainfalls. Because the stratum structure mainly consists of gravelly soil and soil with crushed stones, the water permeability is good. Rainfall is mostly infiltrated into the slope body under the action of gravity, which increases the weight of the slope body, softens the soil body, and affects the stability of the slope body. Silty clay with gravels is distributed within 9.7–17.5 m under the surface of the site. This is the relative water-resisting stratum. The surface water infiltrates and then gathers at the top of the stratum to form the pore water pressure. The pore water pressure produces a buoyancy for the slip mass, influencing the overall stability of the slope. During the rainstorm or continuous rainfall, rainwater is transformed into groundwater through infiltration and then infiltrates into the sliding bed, accelerating the formation of landslide. Therefore, rainfall is a main cause of landslide. At the same time, human engineering activities have a certain promotion effect on the formation of landslide.

At present, the landslide is basically stable in the current working condition, and unstable to less stable in the rainstorm, saturated and seismic conditions. After site leveling, the landslide has multiple levels of sliding surfaces, which are highly possible to be cut out from proposed No. 4 and No. 6 retaining walls. If the landslide isn't controlled, the crack will become wider and longer as the landslide further deforms. When it rains, the surface

water is extremely easy to infiltrate to increase the volume weight of the soil mass. As the deformation of the softened soil layer is exacerbated, the whole landslide is possible to become unstable as a whole to endanger the safety of the proposed dressing plant, with a hazard rating of level 2.

4.3. Landslide control scheme

The disaster body is an unstable slope. The unstable slope prevention and control measures mainly refer to the landslide control methods, which usually include relocation and avoidance, support and anchorage, drainage works, load reduction, and back pressure toe protection

Due to the deformation characteristics and failure mode of the land slide of the 1500t/d Black Bovine Cave Copper Ore Mining & Beneficiation Project Jiulong YalongJiang Mining Co., Ltd., the geological disaster is large in scale, endangers the safety and property safety of over 300 persons, and influences the normal operation of the mine. Therefore, corresponding measures must be taken for prevention and control to ensure safety and economic rationality.

The control scheme for the prevention and control engineering is anti-slide pile + anchor cable + breast board + retaining wall.

4.3.1. Support of anti-slide piles

Anti-slide piles are set to ensure the stability of the soil masses in the middle and back parts of the slope, to prevent the unstable slope soil from being squeezed out by the outer deformed soil mass and inducing uneven settlement of the foundation and basement to destroy the structures of residential houses, and to prevent the downward transmission of the force generated by the soil in the middle and back parts of the slope to help the overall stability of the slope body. According to stability analysis and actual geological survey, the control project has been provided with 64 anti-slide piles for the objects to be protected. This design is divided into sections according to the checked thrust, and the thrust of the tailender sliding block is used for the design and layout. Design is conducted without considering the front resistance of the pile. The totally 8 anti-slide piles designed for No. 2 platform have a section of 1.6×2.4 m, a spacing of 5 m and an average pile length of 30.0 m. An top beam of 0.8×1.2 m is provided on the top of each pile. The length above the sliding surface is 12.8 m, and the depth buried into the rock is 17.2 m. A 0.3 m thick and 12.5 m high baffle is provided between piles. The bottom is embedded into the leveling height by at least 0.5 m. The 3 m long φ 100@2000 drainage holes are embedded in the baffle.

The support scheme of anti-slide piles is HRB400 steel for bars subjected to negative moments and HPB335 steel for stirrups. The pile body is made of C30 concrete, with a 50 mm thick protective layer. Rectangular sections of 1.6×2.4 m and 2.0×3.0 m are used for the sections.

4.3.2. Support of retaining walls

No. 2 retaining wall, located in the excavation area of crude ore bin and coarse crushing chamber, has a platform elevation of 2814.80 m. With a height of 5-6 m and an elevation of 22783.50–783.80 m, the 45.49 m long retaining wall is supported by the down-dip shoulder retaining wall. No. 6 retaining wall, located in the excavation area of pharmaceutical preparation area, has a platform elevation of 2783.80 m and an elevation of 2759.80–2768.80 m. The 5–9 m high and 15 m long retaining wall is supported by the balance-weight retaining wall.

5. Conclusions

This article studies the landslide body control of Black Bovine Cave Copper Ore Mining & Beneficiation Project, with conclusions made below:

1. The landslide at the site of the 1500 t/d Black Bovine Cave Copper Ore Mining & Beneficiation Project is less stable at present. As the influencing factors intensify, the stability will get increasingly worse and the stability of the landslide will gradually decrease, possible to cause sliding failure. It is recommended to control the landslide body in order to ensure the stability of the disaster body, prevent the geological disaster and ensure the smooth completion of mine construction. Therefore it is necessary and urgent to control the landslide body.
2. Landslide stability calculation results show that the landslide after site leveling, with a stability coefficient of 0.849–1.354, is unstable to stable in working. Generally speaking, sliding surfaces A and B of each section have a poor stability, i.e. it is highly feasible to cut out the landslide from No. 4 and No. 6 retaining walls. However, the sliding surface C has a good stability.
3. The comprehensive control measure of "anti-slide pile + retraining wall + baffle + anchor cable" is taken according to analysis. The control scheme can be used to effectively prevent and control the geological disaster, and introduces its engineering layout.

Acknowledgements

This study is supported by the project (Grant No. 2021BCC02003), I gratefully acknowledge this support.

References

[1] B. Rosser, S. Dellow, S. Haubrock, and P. Glassey, "New Zealand's national landslide database", *Landslides*, vol. 14, no. 6, pp. 1949–1959, 2017, doi: 10.1007/s10346-017-0843-6.

[2] R.J. Marin, E.F. Garcia, and E. Aristizabal, "Effect of basin morphometric parameters on physically-based rainfall thresholds for shallow landslides", *Engineering Geology*, vol. 278, art. no. 105855, 2020, doi: 10.1016/ j.enggeo.2020.105855.

[3] R.J. Marin, M.F. Velasquez, and O. Sanchez, "Applicability and performance of deterministic and probabilistic physically based landslide modeling in a data-scarce environment of the Colombian Andes", *Journal of South American Earth*, vol. 108, art. no. 103175, 2021, doi: 10.1016/j.jsames.2021.103175.

[4] T. Gorum and S. Fidan, "Spatiotemporal variations of fatal landslides in Turkey", *Landslides*, vol. 18, no. 5, pp. 1691–1705, 2021, doi: 10.1007/s10346-020-01580-7.

[5] F.W.Y. Ko and F.L.C. Lo, "From landslide susceptibility to landslide frequency: A territory-wide study in Hong Kong", *Engineering Geology*, vol. 242, pp. 12–22, 2018, doi: 10.1016/j.enggeo.2018.05.001.

[6] K. Rana, U. Ozturk, and N. Malik, "Landslide geometry reveals its trigger", *Geophysical Research Letters*, vol. 48, no. 4, art. no. e2020GL090848, 2021, doi: 10.1029/2020GL090848.

[7] A.I. Patton, S.L. Rathburn, D.M. Capps, D. McGrath, and R.A. Brown, "Ongoing landslide deformation in thawing permafrost", *Geophysical Research Letters*, vol. 48, no. 16, art. no. e2021GL092959, 2021, doi: 10.1029/ 2021GL092959.

[8] L. Lombardo, T. Optiz, F. Ardizzone, F. Guzzetti, and R. Huser, "Space-time landslide predictive modelling", *Earth-Science Reviews*, vol. 209, art. no. 103318, 2020, doi: 10.1016/j.earscirev.2020.103318.

[9] V. Kumar, V. Gupta, I. Jamir, and S.L. Chattoraj, "Evaluation of potential landslide damming: Case study of Urni landslide, Kinnaur, Satluj valley, India", *Geoscience Frontiers*, vol. 10, no. 2, pp. 753–767, 2019, doi: 10.1016/j.gsf.2018.05.004.

[10] S. Rezaei, S. Shooshpasha, and H. Rezaei, "Reconstruction of landslide model from ERT, geotechnical, and field data, Nargeschal landslide, Iran", *Bulletin of Engineering Geology and the Environment*, vol. 78, no. 5, pp. 3223–3237, 2018, doi: 10.1007/s10064-018-1352-0.

[11] Z. Bestynski, E. Sieinski, and P. Sliwinski, "Geophysical investigation and the use of their results in the evaluation of the stability of slopes of artificial water reservoirs in the flysch Carpathians", *Archives of Civil Engineering*, vol. 68, no. 3, pp. 71–85, 2022, doi: 10.24425/ace.2022.141874.

[12] A. Duda and T. Siwowski, "Waste tyre bales in road engineering: an overview of applications", *Archives of Civil Engineering*, vol. 67, no. 3, pp. 213–230, 2021, doi: 10.24425/ace.2021.138052.

[13] GB/T 32864–2016 Code for geological investigation of landslide prevention. Standards Press of China, Beijing, 2016 (in Chinese).

Received: 2022-09-03, Revised: 2023-02-07